Superconductivity up to 30 K in the vicinity of the quantum critical point in $BaFe_2(As_{1-x}P_x)_2$

2009 J. Phys.: Condens. Matter 21 382203

(http://iopscience.iop.org/0953-8984/21/38/382203)

IOP FTC
IOP PUBLISHING JOURNAL OF PHYSICS: CONDENSED MATTER
J. Phys.: Condens. Matter **21** (2009) 382203 (5pp) doi:10.1088/0953-8984/21/38/382203

FAST TRACK COMMUNICATION

Superconductivity up to 30 K in the vicinity of the quantum critical point in $BaFe_2(As_{1-x}P_x)_2$

Shuai Jiang[1], Hui Xing[1], Guofang Xuan[1], Cao Wang[1], Zhi Ren[1], Chunmu Feng[2], Jianhui Dai[1], Zhu'an Xu[1] and Guanghan Cao[1,3]

[1] Department of Physics, Zhejiang University, Hangzhou 310027, People's Republic of China
[2] Test and Analysis Center, Zhejiang University, Hangzhou 310027, People's Republic of China

E-mail: ghcao@zju.edu.cn

Received 22 June 2009, in final form 2 July 2009
Published 24 August 2009
Online at stacks.iop.org/JPhysCM/21/382203

Abstract

We report bulk superconductivity induced by an isovalent doping of phosphorus in $BaFe_2(As_{1-x}P_x)_2$. The P-for-As substitution results in shrinkage of the lattice, especially for the FeAs block layers. The resistivity anomaly associated with the spin-density-wave (SDW) transition in the undoped compound is gradually suppressed by the P doping. Superconductivity with a maximum T_c of 30 K emerges at $x = 0.32$, coinciding with a magnetic quantum critical point (QCP) which is shown by the disappearance of SDW order and the linear temperature-dependent resistivity in the normal state. The T_c values were found to decrease with further P doping and no superconductivity was observed down to 2 K for $x \geqslant 0.77$. The appearance of superconductivity in the vicinity of QCP hints at the superconductivity mechanism in iron-based arsenides.

(Some figures in this article are in colour only in the electronic version)

1. Introduction

The discovery of high-temperature superconductivity in iron arsenides [1, 2] was an exciting breakthrough in 2008 [3], which has led to a number of new superconductors [4–6] all containing antifluorite-like FeAs or FeSe layers. In most cases, superconductivity was induced by doping charge carriers into a stoichiometric parent compound which shows a collinear antiferromagnetic spin-density-wave ground state [7]. The chemical doping was initially carried out only outside the FeAs layers, [1, 4, 8, 9] with the electronic phase diagram [10–12] resembling that of cuprate superconductors. Later, however, it was found that even doping at the Fe site (with Co [13] or Ni [14]) could induce superconductivity. Besides, superconductivity was able to be stabilized in the parent compounds simply by applying hydrostatic pressures [15]. The latter two results contrast sharply with those in cuprates.

Very recently, we observed superconductivity at 26 K in $EuFe_2As_2$ by the partial substitution of arsenic with phosphorus [16]. This isovalent substitution does not introduce additional electrons or holes into the system, thus it can be roughly understood in terms of chemical pressures. Owing to the ferromagnetic ordering of Eu^{2+} moments below 20 K coexisting with superconductivity, the Meissner effect was not obvious. Subsequently, we found that the P/As substitution induced superconductivity in a prototype '1111' material LaFeAsO, but the superconducting critical temperature T_c is only ~10 K [17], which is substantially lower than the T_c value under physical pressures [18]. Here we employ the same doping strategy on another prototype '122' parent compound $BaFe_2As_2$ [19]. Bulk superconductivity up to 30 K with strong Meissner diamagnetism has been observed for $x = 0.32$.

[3] Author to whom any correspondence should be addressed.

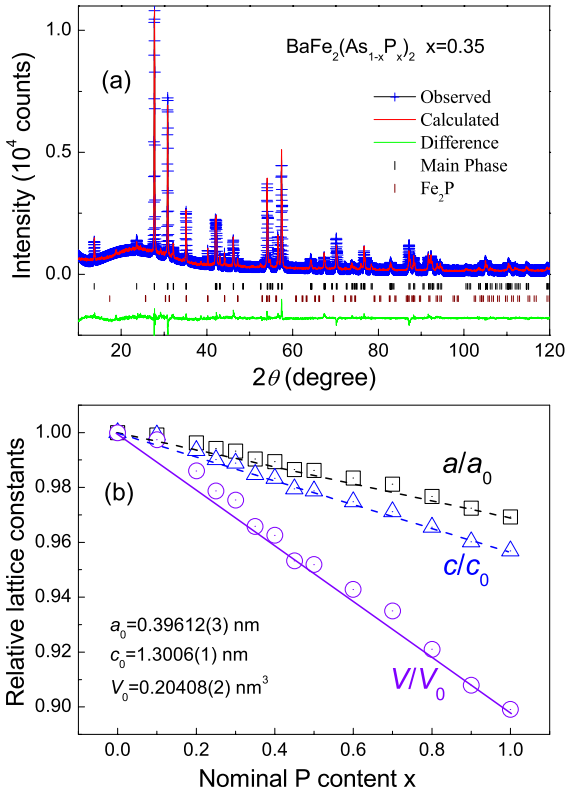

Figure 1. (a) X-ray powder diffraction pattern and its Rietveld refinement profile for the $BaFe_2(As_{1-x}P_x)_2$ ($x = 0.35$) sample. The secondary minor phase is identified as Fe_2P. (b) Relative lattice constants (compared with the undoped compound) as functions of nominal P content x. The solid straight line obeys Vegard's law.

Our systematic measurements of resistivity and magnetization reveal an electronic phase diagram characterized by a dome-like superconducting region located near a magnetic quantum critical point (QCP). The present work is consistent with a recent theoretical prediction which shows a unique type of QCP resulting from a competition between electronic localization and itinerancy [20].

2. Experimental details

Polycrystalline samples of $BaFe_2(As_{1-x}P_x)_2$ (with the nominal P content $x = 0$, 0.1, 0.2, 0.25, 0.3, 0.35, 0.4, 0.45, 0.5, 0.6, 0.7, 0.8, 0.9 and 1) were synthesized by solid-state reaction with the high-purity elements Ba, Fe, As and P. A mixture of the elements in the stoichiometric ratio was pressed into pellets in an argon-filled glove box. The pellets were sealed in evacuated quartz tubes and annealed at 600 K for 12 h, then at 1173 K for 40 h. The resultant was reground, pelletized and annealed in evacuated quartz tubes at 1273 K for 24 h. Finally the samples were cooled down to room temperature by shutting off the furnace.

Powder x-ray diffraction (XRD) was performed at room temperature using a D/Max-rA diffractometer with Cu Kα radiation and a graphite monochromator. The structural refinement was performed using the program RIETAN 2000 [21]. The electrical resistivity was measured using a standard four-probe method. The measurements of dc magnetization were performed down to 1.8 K on a Quantum Design Magnetic Property Measurement System (MPMS-5). Both the zero-field-cooling (ZFC) and field-cooling (FC) protocols were employed under a magnetic field of 10 Oe.

Table 1. Comparison of room-temperature crystal structures between the undoped and P-doped ($x' = 0.32$) $BaFe_2As_2$ with the space group $I4/mmm$. The atomic coordinates are as follows: Ba (0, 0, 0); Fe (0.5, 0, 0.25); As/P (0, 0, z).

Compounds	$BaFe_2As_2$	$BaFe_2(As_{0.68}P_{0.32})_2$
a (Å)	3.9612(3)	3.9231(3)
c (Å)	13.006(1)	12.805(1)
V (Å^3)	204.08(2)	197.08(2)
z of As/P	0.3546(2)	0.3530(2)
FeAs layer thickness (Å)	2.721(2)	2.638(2)
FeAs layer spacing (Å)	3.782(2)	3.765(2)
As–Fe–As angle (deg)	111.0(1)	112.2(1)

3. Results and discussion

The $BaFe_2(As_{1-x}P_x)_2$ system crystallizes in a $ThCr_2Si_2$-type structure with the space group $I4/mmm$. Except for the main phase, a minor secondary phase was identified as Fe_2P. Figure 1(a) shows the XRD pattern and its Rietveld refinement profile of a typical $BaFe_2(As_{1-x}P_x)_2$ sample with $x = 0.35$ at room temperature. The two-phase Rietveld refinement is successful, as indicated by the fairly good reliability factors $R_{wp} = 8.5\%$ and $S = 1.8$. It was found that the fitted P content is a little lower than the nominal one, consistent with the existence of impurity Fe_2P (about 10% in molar ratio). The refined lattice parameters plotted as functions of x are shown in figure 1(b). The cell volume decreases monotonically with the P doping. We notice that, for the samples with no significant Fe_2P impurity (e.g. $x = 0.45$ and 0.9), the data points of the cell volume fall exactly on the straight line, in accordance with Vegard's law. Therefore, the actual P content can be estimated from the measured cell volume, which gives the corrected P content $x' = 0.02$, 0.13, 0.2, 0.24, 0.32, 0.36, 0.47, 0.56, 0.63 and 0.77 for the nominal x values of 0.1, 0.2, 0.25, 0.3, 0.35, 0.4, 0.5, 0.6, 0.7 and 0.8, respectively. This correction is basically (within the uncertainty of ± 0.02) consistent with the Rietveld refinement results.

Table 1 compares the crystal structures between the undoped and P-doped ($x' = 0.32$) $BaFe_2As_2$. A remarkable difference is seen from the position of As/P. The P doping makes the pnictogen atoms move toward the iron sheets, which leads to a dramatic decrease of FeAs layer thickness. This explains why the decrease in the c axis is more pronounced (compared with the a axis), as shown in figure 1(b). In fact, the spacing of FeAs layers decreases little with P doping. This indicates that P doping impacts mainly on the FeAs block layers. As a result, the bond angle of As–Fe–As along [110] directions increases substantially.

Figure 2 shows the temperature dependence of resistivity for $BaFe_2(As_{1-x}P_x)_2$. For the undoped $BaFe_2As_2$, ρ drops rapidly below 140 K, consistent with a previous

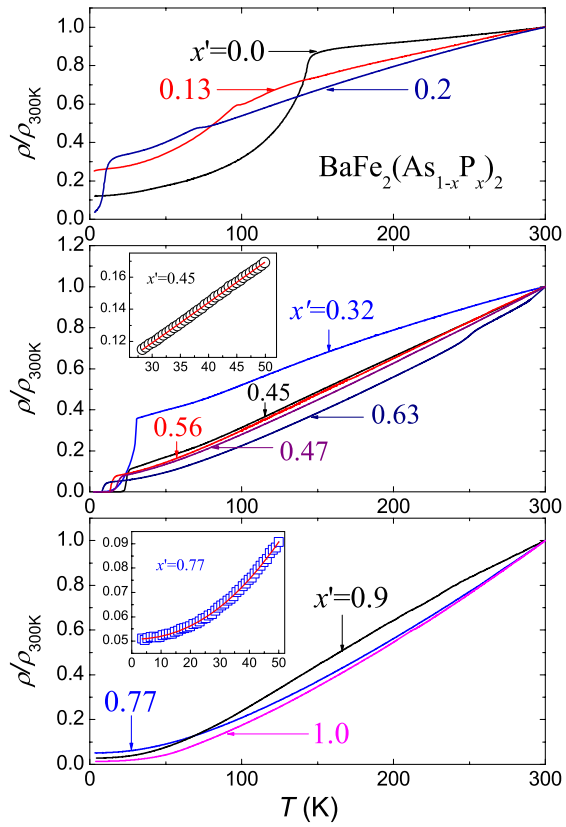

Figure 2. Temperature dependence of resistivity for $BaFe_2(As_{1-x'}P_{x'})_2$ samples. The data are normalized for the convenience of comparison. All the curves are labelled with the corrected P content. The insets display an expanded plot for showing the fit of the normal-state resistivity with the formula $\rho(T) = \rho_0 + \alpha T^n$.

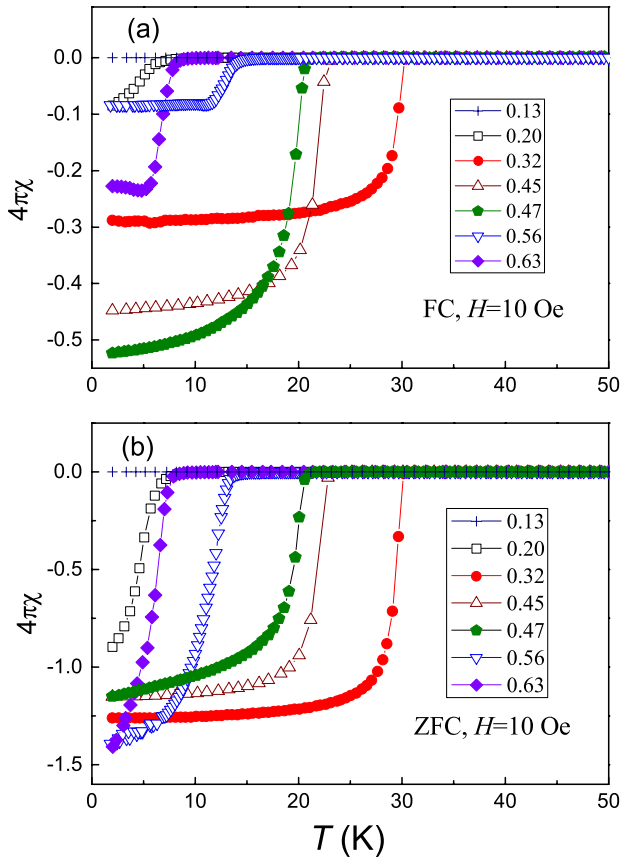

Figure 3. Superconducting diamagnetic transitions in $BaFe_2(As_{1-x'}P_{x'})_2$. Note that the magnetic background coming from the ferromagnetic impurity of Fe_2P has been removed. No correction of demagnetization has been made.

report [19]. The resistivity anomaly was revealed to be associated with a simultaneous structural and spin-density-wave (SDW) transition [22]. Upon doping with P, the transition is suppressed, exhibiting a decrease of transition temperature (T_{SDW}) and a weakening of the resistivity drop. For example, T_{SDW} is suppressed to ~90 K for the sample of $x' = 0.13$, where only a resistivity kink appears. When the P content increases to 20%, a sudden decrease in resistivity is seen below 10 K in addition to an observable kink at ~70 K. The resistivity drop at lower temperature is due to a superconducting transition (confirmed by the magnetic measurements below). In the intermediate doping range ($0.24 \leqslant x \leqslant 0.63$), superconductivity with higher T_cs was observed. The maximum transition temperature is 30 K for $x' = 0.32$. The resistive transition tail is probably due to the influence of grain boundaries and/or minor ferromagnetic Fe_2P impurity, rather than sample inhomogeneity, since nearly perfect diamagnetism was measured (see below). For the higher P doping ($x \geqslant 0.77$), no superconductivity was observed down to 3 K. One notes that the residual resistance ratio (RRR), defined by the ratio of the resistance at room temperature to the residual resistance at very low temperature, is 20, 35 and 75 for $x' = 0.77$, 0.9 and 1.0, respectively. The high RRR values suggest the high quality of the samples.

To confirm superconductivity, the temperature dependence of dc magnetic susceptibility for $BaFe_2(As_{1-x}P_x)_2$ was measured, as shown in figure 3. The sample of $x' = 0.2$ shows a strong diamagnetic transition below 7 K, consistent with the drop in resistivity below 10 K shown in figure 2. In spite of the large superconducting fraction, however, it is difficult to ascertain whether SDW order coexists microscopically with superconductivity or not. For $x = 0.32$, a stronger diamagnetic signal is observed below 30 K. The magnetic shielding is even beyond the ideal value of 100% apparently, since the demagnetization effect is not included here. The Meissner volume fraction achieves ~30%, demonstrating the bulk nature of superconductivity. Other superconducting samples also display a similar bulk property.

As is known, the normal-state resistivity contains valuable information on electronic scattering and even superconducting mechanisms. Dense polycrystalline samples may show an intrinsic transport property because the grain boundaries scatter electrons like impurities. Thus the following analysis is valid even though our data were obtained from polycrystalline samples. Assuming that the intrinsic scattering produces a power-law resistivity at low temperatures, the total resistivity can be expressed as $\rho(T) = \rho_0 + \alpha T^n$, where ρ_0 represents extrinsic resistivity coming from the impurity/defect scattering. By fitting the $\rho(T)$ data in the range of $T_c < T \leqslant 50$ K,

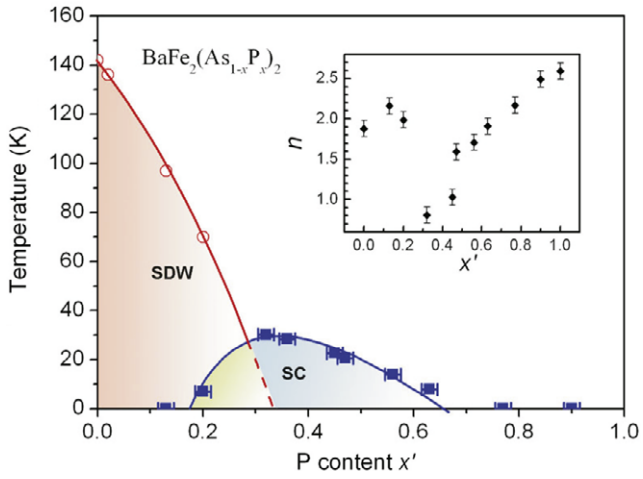

Figure 4. Electronic phase diagram in $BaFe_2(As_{1-x'}P_{x'})_2$. SDW and SC denote spin-density-wave and superconductivity, respectively. The inset shows the variations of the exponent n in the formula $\rho(T) = \rho_0 + \alpha T^n$, obtained by the fitting of normal-state resistivity at low temperatures.

the exponent n was obtained. The inset of figure 4 shows that most samples have the n value close to 2.0, suggesting a Fermi-liquid state due to electron–electron interactions. Interestingly, n is close to unity (i.e. linear T-dependent normal-state resistivity) for the samples with $x' = 0.3$–0.45. The linear low-temperature resistivity belongs to a non-Fermi-liquid behaviour, as usually observed in the regime of quantum criticality. Remembering that the SDW order is suppressed with the P doping, we argue that there exists a QCP at $x' \sim 1/3$ in the $BaFe_2(As_{1-x}P_x)_2$ system. This result is quite consistent with a recent theoretical prediction which shows a unique type of QCP resulting from a competition between electronic localization and itinerancy [20]. We aware that similar QCP was also proposed in the (K, Sr)Fe_2As_2 [12] system.

The electronic phase diagram is concluded in figure 4. The undoped $BaFe_2As_2$ has the ground state of SDW order. With the P doping, T_{SDW} decreases gradually, forming a phase region of SDW. The suppression of SDW can be easily explained in terms of the J_1–J_2 model [23, 24], because J_2 is expected to decrease upon P doping. On the other hand, the scenario of Fermi surface nesting [25] is not quite so straightforward to meet the experimental observation. In the vicinity of the above-mentioned QCP, an asymmetric superconducting (SC) dome emerges. The optimal doping level (with the maximum T_c) coincides with the QCP, where a non-Fermi-liquid behaviour shows up. This strongly suggests that spin fluctuations play an important role for the superconductivity. In the overlapped area of SDW and SC, it is not clear whether SDW coexists microscopically with SC at this moment. The upper-right metallic region displays a Fermi-liquid-like state, except that non-Fermi-liquid behaviour appears near the QCP. This crossover in electronic excitation states resembles those of the (K, Sr)Fe_2As_2 [12] and $Ba(Fe_{1-x}Co_x)_2As_2$ [26] systems.

It was reported that $BaFe_2As_2$ became superconducting up to 29 K under the high pressure of ~4 GPa [27]. The T_c value is very close to the present one in $BaFe_2(As_{1-x}P_x)_2$. This implies that chemical pressure generated by P doping acts in a similar way to the physical pressure. Meanwhile, the disorder induced by the P doping hardly influences superconductivity. The relatively low T_c^{max} value (compared with 38 K in $Ba_{0.6}K_{0.4}Fe_2As_2$ [4]) can be well understood by an empirical structural rule for T_c variations [11]. Very recent work [28] also reveals similarities between structural distortions under pressure and chemical doping in $BaFe_2As_2$. Therefore, it is the structural details of FeAs layers (corresponding to specific electronic structures), rather than charge doping level, that controls the ground states in iron arsenides.

To summarize, $BaFe_2As_2$ has been turned superconducting through an isovalent doping of phosphorus at the arsenic site, for the first time. Unlike a previous doping strategy of changing the concentration of charge carriers, the present P doping does not alter the number of valence electrons. Structural measurements indicates that the chemical pressure generated by the P doping impacts mainly on the FeAs layers. The P-for-As substitution suppresses the SDW ordering and favours superconductivity, similarly to the phenomena of carrier doping [4, 10, 11]. A magnetic QCP is shown simultaneously by the disappearance of SDW ordering and the non-Fermi-liquid behaviour. The maximum T_c of 30 K is observed where the QCP is located. Theoretical studies [29] indicate that superconductivity around a magnetic QCP is associated with the spin fluctuation mechanism. Thus the present result suggests that spin fluctuations play a crucial role for the superconductivity in iron-based arsenides.

Acknowledgments

This work is supported by the NSF of China (no. 10674119), the National Basic Research Programme of China (no. 2007CB925001) and the PCSIRT of the Ministry of Education of China (IRT0754).

References

[1] Kamihara Y, Watanabe T, Hirano M and Hosono H 2008 *J. Am. Chem. Soc.* **130** 3296
[2] Chen X H, Wu T, Wu G, Liu R H, Chen H and Fang D F 2008 *Nature* **453** 761
[3] The Editorial 2008 Breakthrough of the year *Science* **322** 1770
[4] Rotter M, Tegel M and Johrendt D 2008 *Phys. Rev. Lett.* **101** 107006
[5] Wang W C *et al* 2008 *Solid State Commun.* **148** 538
Pitcher M J *et al* 2008 *Chem. Commun.* 5918
Tapp J H *et al* 2008 *Phys. Rev.* B **78** 060505(R)
[6] Hsu F C *et al* 2008 *Proc. Natl Acad. Sci.* **105** 14262
[7] Cruz C *et al* 2008 *Nature* **453** 899
[8] Wang C *et al* 2008 *Europhys. Lett.* **83** 67006
[9] Wen H H *et al* 2008 *Europhys. Lett.* **82** 17009
[10] Liu R H *et al* 2008 *Phys. Rev. Lett.* **101** 087001
[11] Zhao J *et al* 2008 *Nat. Mater.* **7** 953
[12] Gooch M, Bing L, Lorenz B, Guloy A M and Chu C W 2009 *Phys. Rev.* B **79** 104504
[13] Sefat A S *et al* 2008 *Phys. Rev.* B **78** 104505
Wang C *et al* 2009 *Phys. Rev.* B **79** 054521
[14] Cao G H *et al* 2009 *Phys. Rev.* B **79** 174505
Li L J *et al* 2009 *New J. Phys.* **11** 025008
[15] Torikachvili M S *et al* 2008 *Phys. Rev. Lett.* **101** 057006

Park T *et al* 2008 *J. Phys.: Condens. Matter* **20** 322204
[16] Zhi R *et al* 2009 *Phys. Rev. Lett.* **102** 137002
[17] Wang C *et al* 2009 *Europhys. Lett.* **86** 47002
[18] Okada H *et al* 2008 *J. Phys. Soc. Japan* **77** 113712
[19] Rotter M *et al* 2008 *Phys. Rev.* B **78** 020503(R)
[20] Dai J H, Si Q M, Zhu J X and Abrahams E 2009 *Proc. Natl Acad. Sci.* **106** 4118
[21] Izumi F *et al* 2000 *Mater. Sci. Forum* **321–324** 198
[22] Huang Q *et al* 2008 *Phys. Rev. Lett.* **101** 257003
[23] Si Q and Abrahams E 2008 *Phys. Rev. Lett.* **101** 076401
[24] Yildirim T 2008 *Phys. Rev. Lett.* **101** 057010
[25] Dong J *et al* 2008 *Europhys. Lett.* **83** 27006
[26] Wang X F *et al* 2009 *New J. Phys.* **11** 045003
[27] Alireza P L *et al* 2008 *J. Phys.: Condens. Matter* **21** 012208
[28] Kimber S A *et al* 2009 *Nat. Mater.* **8** 471
[29] Moriya T and Ueda K 2003 *Rep. Prog. Phys.* **66** 1299